

Review

# Gallate-Based Metal–Organic Frameworks, a New Family of Hybrid Materials and Their Applications: A Review

Marhaina Ismail <sup>1</sup>, Mohamad Azmi Bustam <sup>1,2,\*</sup>  and Yin Fong Yeong <sup>1</sup>

<sup>1</sup> Carbon Dioxide Research Centre (CO2RES), Universiti Teknologi PETRONAS, Perak 32610, Malaysia; marhaina\_19001049@utp.edu.my (M.I.); yinfong.yeong@utp.edu.my (Y.F.Y.)

<sup>2</sup> Centre of Research in Ionic Liquids (CORIL), Universiti Teknologi PETRONAS, Perak 32610, Malaysia

\* Correspondence: azmibustam@utp.edu.my

Received: 1 October 2020; Accepted: 26 October 2020; Published: 5 November 2020



**Abstract:** Within three decades of fundamental findings in research on metal–organic frameworks (MOFs), a new family of hybrid materials known as gallate-based MOFs, consisting of metal salt and gallic acid, have been of great interest. Due to the fact that gallic acid is acknowledged to display a range of bioactivities, gallate-based MOFs have been initially expended in biomedical applications. Recently, gallate-based MOFs have been gradually acting as new alternative materials in chemical industrial applications, in which they were first reported for the adsorptive separation of light hydrocarbon separations. However, to date, none of them have been related to CO<sub>2</sub>/CH<sub>4</sub> separation. These porous materials have a bright future and can be kept in development for variety of applications in order to be applied in real industrial practices. Therefore, this circumstance creates a new opportunity to concentrate more on studies in CO<sub>2</sub>/CH<sub>4</sub> applications by using porous material gallate-based MOFs. This review includes the description of recent gallate-based MOFs that presented remarkable properties in biomedical areas and gas adsorption and separation, as well as their future potential application.

**Keywords:** metal–organic frameworks; gallate-based MOFs; gallic acid; CO<sub>2</sub>

## 1. Introduction

A metal–organic framework (MOF) is a porous hybrid organic-inorganic material that has a strong coordination bond between a node (metal) and organic linker. MOFs are comprised of metal-containing nodes that bond to organic linkers which results in well-defined crystalline structures [1]. MOFs can be practically designed and synthesized according to the building blocks that join together to build a framework [2]. Through the selection of suitable building blocks during synthesis, these porous materials with different shapes and functionalities can be designed for various applications [3]. The three-dimensionally ordered framework structures can make MOFs sufficiently robust to permit the removal of the adsorbed guest species, giving rise to permanent porosity [4]. The first MOFs with permanent porosity were introduced in 1995 by Yaghi and Li [5]. The great interest in designing novel MOFs is gradually growing, due to their exclusive structural and functional properties. Among the previously studied MOFs are MOF-74 [6], MOF-177 [7], MOF-5 [8], ZIF-8 [9], HKUST-1 [10], MIL-101 [11], IRMOF-1 [12], UiO-66 [13], Nu-1000 [14], MFU-4 [15], NOTT-300 [16], and so on. In addition, MOFs are widely synthesized using the solvothermal method, with extensive washing process in order to maximize the effective pore activation [17].

As a rising class of porous material, MOFs have gained worldwide attention, owing to their unique properties such as high surface area and pore volume, well-ordered porous structure, multiple reaction

sites, easily tailored structures, and diverse means available for functionalization [18,19]. MOFs can also contribute to several significant roles as selective adsorbents. This is due to the fact that MOFs have large pore sizes which enable rapid diffusion kinetics, tunable binding strengths that can affect adsorption selectivity, and, also, high surface areas that can bring large working capacity [20]. Therefore, MOFs are promising agents for adsorption/separation [21], energy storage [22], drug delivery [23], catalysis [24], magnetism [25], luminescence [26], sensors [27], and other useful applications [28].

Despite all the given advantages of MOFs, the major drawback for commercialization and industrial applications is the cost of MOFs, which will affect the scale-up production of MOFs on a long-term basis [29]. The choice of raw materials notably impacts large-scale production, because the price per kg of the final MOF products must meet the lowest possible price in order to be economically viable [30]. Linker is one of the most expensive materials in the production of MOFs, since it can reach up to 40% of the total production costs [31]. Gallic acid is known to have advantages over expensive organic linker due to low cost, low toxicity, easy availability, and natural abundance [32]. The previous study has already proven that gallic acid can act as a successful alternative organic linker in a new family of hybrid framework materials known as gallate-based MOFs or M-gallate [33]. This gallic acid is gained from the industrial-scale production of biomass and cost around USD 10/kg [34]. In addition, the entire synthetic process is environmentally friendly without the consumption of organic solvents [35]. Nonetheless, very few studies have been conducted on the applications of gallate-based MOFs in industry, as they have just started to gain recognition. At first, gallate-based MOFs were widely used in biomedical applications. A couple of years back, gallate-based MOFs gradually gained attention in small scopes of chemical applications, such as light hydrocarbon separations, due to their outstanding performance. Thus, gallic acid has the potential to be an excellent organic linker for gallate-based MOFs due to its environmentally and economically friendly nature.

### 1.1. Gallic Acid

Gallic acid is classified as a phenolic compound, chemically named as 3,4,5-trihydroxybenzoic acid [36,37]. The molecular dimension of gallic acid is a planar molecule, comprising of an aromatic ring surrounded by three hydroxyl groups and a carboxyl group [38,39]. This compound is a potential organic linker in forming organic frameworks, due to the availability of five oxygen atoms located at the opposite side of the molecule, in which there are slightly large gaps between the phenolic oxygens that are capable of chelating metal ions [40]. The other name of gallic acid is gallate, and its chemical structure ( $C_7H_6O_5$ ) is shown in Figure 1.

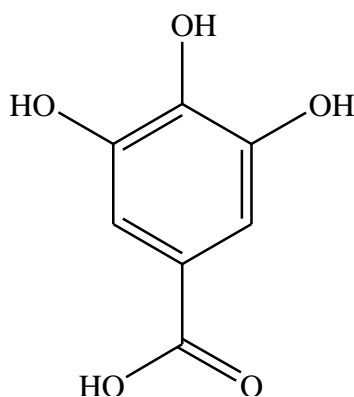


Figure 1. Structure of gallic acid.

Polyphenols are known as secondary compounds and commonly found in the plant kingdom classified into four classes such as phenolic acids, flavonoids, stilbenes and lignans [41]. Phenolic compounds are essential for the main organoleptic characteristics of plant-derived foods and beverages, specifically for color and taste properties [42]. Phenolic acids are a diverse group reported

from plants that consist of ferulic acid, synergic acid, ellagic acid, caffeic acid and so on [36]. One of the phenolic acids is gallic acid, which is available in various fruits, vegetables, wine, coffee and tea [36]. Gallic acid that can be found in plants is in the form of esters, free acids, hydrolysable tannins and catechin derivatives [36].

Gallic acid is a slightly colorless/yellow crystalline solid with melting point of 210 °C, and decomposition within the temperature range 235–240 °C [43]. It is soluble in water, ether, alcohol and glycerol, but insoluble in chloroform, benzene and ether petroleum [43]. In addition, this organic linker can form stable complexes with transition metal ions such as Fe(III), Co(II), Mn(II), Ni(II), Zn(II), Cu(II), and Cd(II) [38].

Gallic acid and its derivatives are considered to be natural products of the hydrolysis of tannins that are commonly found in plants such as green and black teas, oak, pomegranate husk and grape [44]. For practical applications, gallic acid is prepared through the breakdown of tannic acid by an enzyme known as tannase, a glycoprotein esterase [43]. The huge interest in this compound is due to its various biological effects, including anti-allergic [45], anti-inflammatory [46], antiviral [47], antifungal [48], antimicrobial [37], antimutagenic [49], cardioprotective [50], neuroprotective [51], and anticarcinogenic activities [52].

## 1.2. Gallate-Based MOFs

Gallate-based MOFs, designated as M-gallate, have gained researchers' attention due to the easily accessible nature of gallic acid and their uncomplicated preparation [53]. These frameworks, that are prepared from the reaction of metal salts and gallic acid, will give chemical formulas of  $M(C_7O_5H_4) \cdot 2H_2O$  for divalent cations, and  $M(C_7O_5H_3) \cdot 2H_2O$  for trivalent cations [33]. One of the significant characteristics of the gallate-based MOFs is that they can contain both divalent and trivalent cations by maintaining the charge balance [40]. Gallate-based MOFs, such as  $Fe(C_7H_3O_5) \cdot 2H_2O$  and  $M(C_7H_4O_5) \cdot 2H_2O$ , ( $M = Mn^{2+}, Co^{2+}, Ni^{2+}$ ), are intriguing in this aspect, since they are inorganically bonded chains and also have the possibility to exhibit mixed valency through a process named cation doping [33]. In addition, gallate-based MOFs have been proven to have high stability against water and oxygen, as well as recyclability, since they can be applied under repetitive adsorption–desorption cycles which are important for real-world applications [54].

Figure 2 shows the crystal structure of gallate-based MOFs, which was reported by a previous work [35]. M, C, O and H are highlighted in purple, black, red and white, respectively. Based on this research, the crystal structure contained the infinite chains of corner-sharing distorted  $MO_6$  octahedra, coordinated via the organic linkers (four O atoms from the phenolic hydroxyls of two different linkers, and two O from the carboxyls of another two linkers) [35]. The regular main channels can be found due to the spiral extension of the connection of metal octahedra and organic linkers around the c axis, along with regular branched channels leaning against the main ones [35].

Gallate-based MOFs have been known since antiquity, in which iron gallate has been used as an ink and a dye due to its strong absorption in the visible region [40]. This pioneering application of gallate-based MOFs was introduced in historical iron gall ink (iron gallate) as a writing material. This kind of ink was used to record various necessary documents and drawings in human history, such as hand-written works [55]. Despite its historical interest, the chemical structure and composition have been subjects of concern. Hence, the study of its crystal structure performed in 1991 disclosed that it was a 1-D hybrid metal oxide, consisting of infinite chains of *trans*-corner-sharing  $FeO_6$  octahedra [56]. The historical colorant of iron gall ink resulted from a reaction of aqueous Fe(II) and gallic acid, resulting in an iron-gallate complex study [57]. Apart from that, the other early application of these solids can be found in the utilization of the lanthanide gallate-based compounds, which were used as the substrates for the thin film growth of superconductors [58]. Thus, the study regarding gallate-based MOFs has been progressed steadily throughout the years to illustrate their synthesis, crystal structures, magnetic properties, and thermal behavior [33,40].

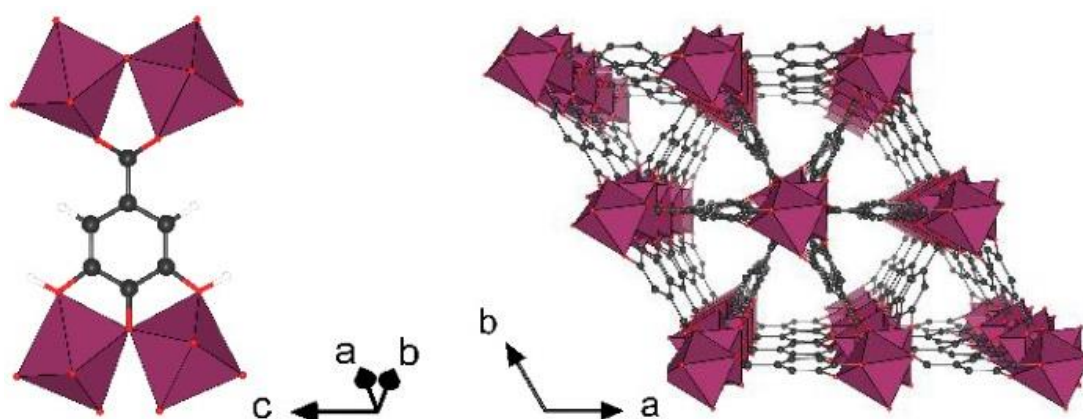


**Figure 2.** Crystal structure of gallate-based metal–organic frameworks (MOFs). Reprinted with permission [35].

## 2. Biomedical Applications

Due to the various biological effects of gallic acid, gallate-based MOFs have been further applied in biomedical applications such as antioxidant carrier and anticancer agent. This is well coincided, since biomedical applications have recently appeared as one of the most engaging among the potential uses of MOFs [59]. Most MOFs are biodegradable, and their stability range is from less than a few hours up to several weeks, which can reduce their accumulation in the body [60].

### 2.1. Antioxidant Carrier

A previous study has proclaimed that biocompatible magnesium-gallate (Mg-gallate) can act as an antioxidant carrier [61]. In this work, microporous Mg-gallate ( $\text{Mg}(\text{C}_7\text{O}_5\text{H}_4) \cdot 2\text{H}_2\text{O}$ ) is formed from biocompatible materials to evaluate its antioxidant activity by slowly releasing gallic acid when this microporous solid degraded in physiological fluids (water and cell culture medium RPMI). Mg-gallate is comprised of gallic acid, which is a natural linker, and Mg(II) is the cation that has already been applied in the preparation of several preferred MOFs. This cation also played an important role in resisting the oxidative stress, which brought extra advantages when incorporated with antioxidative species. Initially, MOFs are designed for controlled drug release, mostly through physisorption processes. Recently, a promising alternative is proposed which is the combination of the active molecule within the framework and its release by degradation of the framework itself. Prior to conventional physisorption processes, this method is utilized for the release of a higher amount of active molecule (in wt. %). In addition, this method can also release kinetics dependent on the degradation rate, while preventing the usage of exogenous compound of unidentified toxicity. It can be proven that Mg-gallate can act as a controlled release source of gallic acid into both physiological fluids, which is it is faster in RPMI (48% after 24 h) than in water (37% after 24 h). The antioxidant properties of Mg-gallate are measured on the HL-60 cell line by the production of Reactive Oxygen Species (ROS). Therefore, Mg-gallate is not only slowly releasing gallic acid by degrading in physiological fluids, but can also result in strong antioxidant activity.

The continuation of the aforementioned study is conducted by discovering the reactivity of gallic acid with another non-toxic cation (calcium) to evaluate the influence of the composition and structure on the bioactivity of these materials [62]. In this extended work, two proposed calcium gallate frameworks, designated as MIL-155 and MIL-156 (MIL is Materials Institute Lavoisier), have been hydrothermally synthesized, and these porous materials are incorporated on different inorganic subunits. MIL-155 ( $[\text{Ca}_2(\text{H}_2\text{O})(\text{H}_2\text{gal})_2] \cdot 2\text{H}_2\text{O}$ ) and MIL-156 ( $[\text{Ca}_3\text{K}_2(\text{H}_2\text{O})_2(\text{gal})_2] \cdot n\text{H}_2\text{O}$ ) exhibited different compositions and crystal structures, even though both of them are made from the same constituents, which caused them to have significant different in solubility profiles, specifically in simulated biological media, and, therefore, distinct biological activities. The potential antioxidant

activities of MIL-155 and MIL-156 are also measured by the production of Reactive Oxygen Species (ROS). It is reported that MIL-156 did not exhibit any antioxidant effect due to its high chemical stability. Meanwhile, MIL-155 exhibited a significant protective antioxidant effect, which was higher than that of Mg-gallate (previously reported).

## 2.2. Anticancer Agent

Over the past few years, MOFs have been developed as the outstanding agents in drug delivery for treating diseases such as cancer [63]. The previous work has provided information about the synthesis of photosensitizer-incorporated copper gallate nanoscale metal–organic framework (Cu-GA NMOF) for the codelivery of anticancer agent to cancer cells [64]. Anticancer agent (gallic acid) is integrated in the framework as an organic linker and then, the photosensitizer methylene blue (MB) is postsynthetically loaded to the framework, resulting in concurrent light-activated photodynamic therapy *in vitro* and *in vivo*. Therefore, this material appeared to be the carrier of two anticancer agents, by the gallic acid and photosensitizer methylene blue. The photosensitizer MB-loaded Cu-GA NMOF has been well applied for the synergy of anticancer drug delivery and photodynamic therapy in cells *in vitro*. In addition, the tumor regression curve *in vivo* disclosed that MB-loaded Cu-GA NMOF, in combination with photo-irradiation of the tumor, brought about a remarkable decrement of the tumor burden due to the mutual effects of controlled ROS generation and photodynamic therapy. MB-loaded Cu-GA NMOF has been proven to act in the codelivery of anticancer agent (gallic acid) and photosensitizer (methylene blue) to cancer cells. Therefore, this material is considered as a new potential nanomaterial for *in vivo* preclinical cancer phototherapy applications.

## 3. Chemical Industrial Applications

The purification and separation processes are crucial in the chemical industry. Among these, the purification and separation of gas mixtures are of great interest, such as natural gas sweetening ( $\text{CO}_2/\text{CH}_4$ ), hydrogen purification ( $\text{H}_2/\text{N}_2$ ,  $\text{H}_2/\text{CO}$ ,  $\text{H}_2/\text{CO}_2$ ,  $\text{H}_2/\text{hydrocarbons}$ ),  $\text{CO}_2$  capture ( $\text{CO}_2/\text{air}$ ,  $\text{CO}_2/\text{H}_2$ ), air separation ( $\text{N}_2/\text{O}_2$ ), and hydrocarbon separation (olefins/paraffins, linear/branched isomers) [65]. Hydrocarbon separation signifies as an essential petrochemical process, both for feedstock production and the end products preparation [66]. Typically, the hydrocarbon mixture separations are accomplished by an energy and capital-intensive process known as cryogenic distillation. This process requires a number of distillation stages and a high reflux ratio in order to prepare the feedstock or end product, in which the process must be carried out at the certain cryogenic temperature and at a high pressure [66]. Therefore, it is necessary to develop a promising alternative technology that offers potential energy saving with lower capital and operating costs.

Adsorption using porous solids is acknowledged as a potential alternative separation process, where the guest molecules are adsorbed into the pores of the solids and desorbed as a function of temperature or pressure [66]. MOFs have been established as a developing class of materials that are valuable in gas capture, gas storage, gas purification, and gas separation applications [67–69]. This is due to the fact that MOFs are greatly driven by the quest for porosity and large surface area, making MOFs promising candidates in those applications [30,70]. In addition, MOFs have been chosen to be the potential candidates for the adsorptive separation of light gas molecules due to the structural diversity and designable pore properties, as well as the significant role pore aperture plays in adsorption separation [54]; for example, the adsorptive separation of acetylene/ethylene [71], ethane/ethylene [72], propane/propylene [73], carbon dioxide/acetylene [74], and several other gases. Gas separation using MOFs mainly depended on the size of the pores as well as the affinity of MOFs towards the targeted molecules [75]. Purification and separation processes are essential for the chemical industry in order to separate the pure components from chemical mixtures [76]. Therefore, gallate-based MOFs have gradually attracted researchers' interest in chemical industrial applications, particularly for light hydrocarbon separations.

### 3.1. Adsorptive Separation of Ethylene from Ethylene/Ethane Mixture

Ethylene is one of the main raw materials in the petrochemical industry that is produced by ethane and naphtha cracking processes, forming a mixture of ethylene and un-cracked ethane [77]. This type of separation is among the most essential and challenging industrial separation processes, and is generally achieved through the energy-intensive cryogenic distillation [78]. The first ever application of gallate-based MOFs for light hydrocarbon separation is in the adsorptive separation of ethylene from ethylene/ethane mixture [35]. In this work, gallate-based MOFs, M-gallate ( $M(C_7O_5H_4) \cdot 2H_2O$ ,  $M = Ni, Mg, Co$ ) are reported for the molecular sieving of ethylene and ethane through the molecular cross-section size differentiation. Through using the appropriate pore sizes and geometries for size or shape sieving, the ideal porous materials for certain separation are determined, in which they are able to capture the smaller molecules while blocking the larger ones. The schematic diagram in Figure ?? shows the limiting aperture size of gallate-based MOFs ( $3.47 \text{ \AA} \times 4.85 \text{ \AA}$  for Ni-gallate,  $3.56 \text{ \AA} \times 4.84 \text{ \AA}$  for Mg-gallate and  $3.69 \text{ \AA} \times 4.95 \text{ \AA}$  for Co-gallate), which is well-fitted with the minimum cross-section size of ethylene ( $3.28 \text{ \AA} \times 4.18 \text{ \AA}$ ), but smaller than the minimum cross-section size of ethane ( $3.81 \text{ \AA} \times 4.08 \text{ \AA}$ ). It shows that ethylene molecules can pass through the pore while ethane molecules are prevented from entering the pore channel.

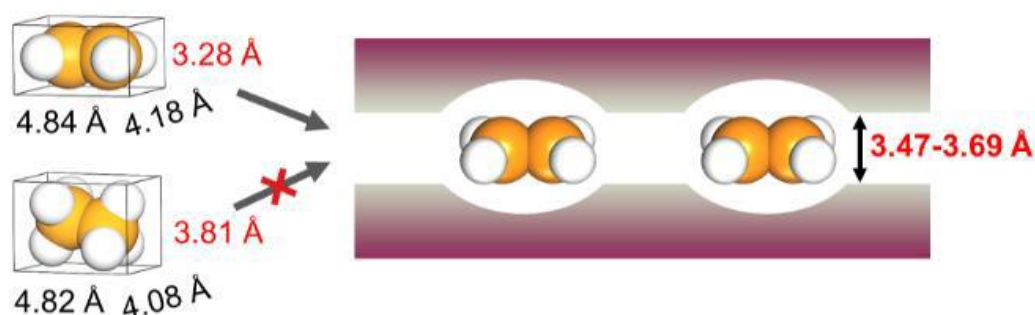


Figure 3. Schematic diagram of molecular sieving of ethylene and ethane. Reprinted with permission [35].

Therefore, these gallate-based MOFs are capable of selectively adsorbing ethylene while blocking ethane due to the perfect aperture dimension falling within the range of the minimum cross-section size of ethylene and ethane, which leads to the high selectivity of ethylene over ethane. The highest ethylene (single component) uptake is achieved by Co-gallate, with 3.37 mmol/g at 298 K and 1 bar conditions, followed by Mg-gallate and Ni-gallate with 3.03 and 1.97 mmol/g, respectively. Based on the comparison, it can be concluded that the slight enlargement of the pore aperture from Co-gallate to Ni-gallate has enabled higher ethylene uptake and made Co-gallate reach the top of the list as it has a slightly larger pore size compared to Mg-gallate and Ni-gallate. It is worth noting that all M-gallate MOFs are capable of excluding ethane molecules from entering the pore, as the ethane (single component) uptake is low, with values of 0.31, 0.28 and 0.26 being achieved by Co-gallate, Ni-gallate and Mg-gallate, respectively.

Most importantly, Co-gallate displayed a remarkable Ideal Adsorbed Solution Theory (IAST) selectivity of 52 for the equimolar ethylene/ethane mixtures, which was followed by Mg-gallate and Ni-gallate, with 37.3 and 16.8, respectively, at 298 K and 1 bar conditions. In relation to the breakthrough experiment of equimolar ethylene/ethane mixtures, this work also showed that the studied gallate-based MOFs are highly selective for ethylene, which is proven by a significantly delayed breakthrough of ethylene compared to ethane. Therefore, this work demonstrated that gallate-based MOFs are potential materials for the adsorptive separation of ethylene and ethane.

### 3.2. Adsorptive Separation of Acetylene from Acetylene/Ethylene Mixture

The separation of acetylene from an acetylene/ethylene mixture is an important industrial process, as acetylene can have a destructive effect on the product line of ethylene [79]. The conventional

technologies for the removal of acetylene, such as partial hydrogenation or cryogenic distillation, are cost-intensive and energy-intensive processes, and, therefore, adsorptive separation using a porous solid has been chosen as an alternative energy-efficient solution [80]. A study has demonstrated that gallate-based MOFs, namely M-gallate ( $M(C_7O_5H_4) \cdot 2H_2O$ ,  $M = Ni, Mg, Co$ ), not only display outstanding separation performance for the removal of acetylene from ethylene, but also surprisingly increased the ethylene productivity [54]. In this work, the reported gallate-based MOFs can excellently tune the pore size by substituting the different metal species, thus having a remarkable impact on the separation performance of acetylene/ethylene adsorption. Owing to the similar properties of the six coordinated metal ions, the small radius difference ( $Co^{2+} = 88.5$  pm,  $Mg^{2+} = 86.0$  pm and  $Ni^{2+} = 83.0$  pm) made it possible to tune the aperture sizes of gallate-based MOFs, due to the small difference in the metal-oxygen bond length. The minimum pore aperture sizes of gallate-based MOFs ( $3.47 \text{ \AA} \times 4.85 \text{ \AA}$  for Ni-gallate,  $3.56 \text{ \AA} \times 4.84 \text{ \AA}$  for Mg-gallate and  $3.69 \text{ \AA} \times 4.95 \text{ \AA}$  for Co-gallate) are theoretically perfect for the adsorption separation of acetylene/ethylene, as the kinetic diameter for both acetylene and ethylene are  $3.3 \text{ \AA}$  and  $4.16 \text{ \AA}$ , respectively.

Single-component adsorption isotherms of Ni-gallate, Co-gallate and Mg-gallate for acetylene uptake showed 80.4, 87.1 and 98.4  $cm^3/g$ , respectively, at 289 K and 1 bar conditions. Among the studied metal ions, Ni-gallate has the smallest radius, and therefore exhibited the narrowest aperture size, and consequently gave the lowest acetylene uptake. It can be stated that the smaller the radii of the metal ions, the shorter the metal-oxygen bonds of gallate-based MOFs. As a result, a lower capacity of acetylene is produced. By contrast, Mg-gallate showed higher acetylene uptake compared to Co-gallate, despite having a lower aperture size due to the stronger binding affinity, which is caused by the larger electrostatic interactions between the Mg-gallate structure and the more delocalized charge in the acetylene gas.

It can also be found that Co-gallate, Mg-gallate and Ni-gallate demonstrated remarkable performance for the equimolar acetylene/ethylene mixtures, with IAST selectivity of 13.7, 20.3 and 56.7, respectively, at 289 K and 1 bar conditions. Since Ni-gallate gave the highest selectivity, it displayed the longest retention time of acetylene up to 408 min/g in the fixed bed, followed by Mg-gallate and Co-gallate with 384 min/g and 224 min/g, respectively. Meanwhile, ethylene underwent breakthrough at the start of the experiment, at about 32 min/g for Mg-gallate, 45 min/g for Co-gallate and 36 min/g for Ni-gallate, illustrated the weak affinity of the M-gallate frameworks towards ethylene. Therefore, these facts explained the excellent ability for capturing acetylene, and the outstanding adsorption selectivity in terms of acetylene/ethylene separation. This work has shown that varying the metal ions in gallate-based MOFs can produce significant changes in gas separation behavior. These materials, which are synthesized from inexpensive gallic acid, can act as promising adsorbents in the purification of ethylene from the ethane and naphtha cracking processes.

### 3.3. Adsorptive Separation of Geometric Isomers of 2-Butene

$C_4$  olefins are crucial feedstock for the production of synthetic rubbers or other chemical products [81]. The separation of  $C_4$ -olefins mixtures by distillation in the chemical industry is difficult and highly energy-intensive, owing to the close boiling points of the unsaturated  $C_4$  isomers [82]. Among these geometric isomers, the separation of *trans/cis*-2-butene is the most challenging process, and it is really important to enhance the added-value of  $C_4$ -olefins [83]. Gallate-based MOFs are also proven to act as promising porous materials in the adsorptive separation of geometric isomers of 2-butene [83]. In this work, gallate-based MOFs, M-gallate ( $M(C_7O_5H_4) \cdot 2H_2O$ ,  $M = Ni, Mg, Co$ ) are reported for the shape-selective separation of *trans/cis*-2-butene through their differentiation in minimum molecular cross-section size. Based on Figure 4, the pore size of Mg-gallate ( $3.6 \text{ \AA} \times 4.6 \text{ \AA}$ ) is smaller than the minimum cross-section size of *cis*-2-butene ( $3.6 \text{ \AA} \times 4.9 \text{ \AA}$ ) but slightly larger than the minimum cross-section size of *trans*-2-butene ( $3.5 \text{ \AA} \times 4.6 \text{ \AA}$ ). As a result, *trans*-2-butene can pass through and be suitably captured in the oval-shaped pore channel, while *cis*-2-butene is excluded from the pore.

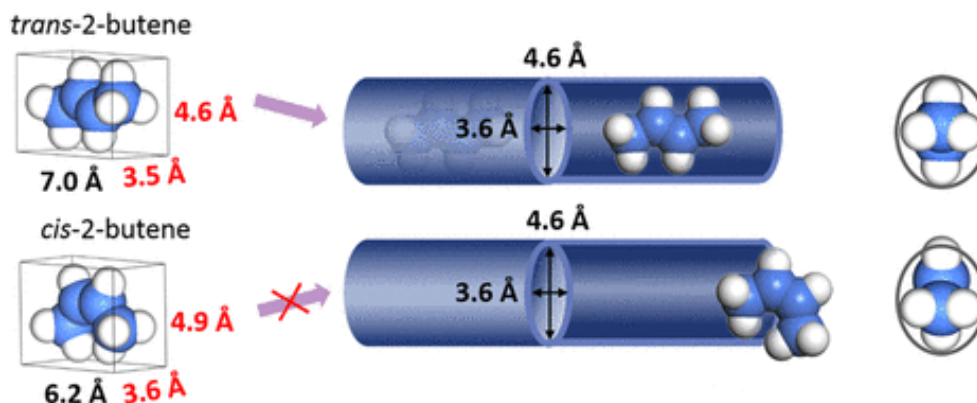


**Figure 4.** Schematic diagram of shape-selective separation of *trans*-2-butene and *cis*-2-butene. Reprinted with permission [83].

Mg-gallate displayed the highest *trans*-2-butene uptake at 298 K and 1 bar conditions, which was 1.85 mmol/g, followed by Co-gallate and Ni-gallate, with 1.67 and 1.09 mmol/g, respectively. The low affinity between the frameworks and *cis*-2-butene is proven by the low *cis*-2-butene uptake, which was 0.58 mmol/g for both Mg-gallate and Co-gallate, and 0.44 mmol/g for Ni-gallate. Surprisingly, Mg-gallate showed the record of the highest *trans/cis*-2-butene selectivity, of 3.2 at 298 K and 1 bar in the single-component adsorption isotherm, followed by Co-gallate and Ni-gallate with 2.9 and 2.5, respectively. This work demonstrated that gallate-based MOFs are potential industrial materials for the adsorption separation of geometric isomers of C<sub>4</sub> hydrocarbons. In addition, this work also provided significant information for other hydrocarbon isomer separations.

#### 3.4. Adsorptive Separation of Propyne from Propylene/Propylene Mixture

Propylene is a prime olefin raw material for petrochemical production and important feedstock for the manufacture of various chemicals such as polypropylene [84]. Propylene is mainly produced by steam-cracking of hydrocarbons, and there is unavoidably propyne trace generated during the production process [85]. The removal of propyne trace from propylene is essential for the production of polymer-grade propylene [34]. The conventional approach for the removal of propyne trace is greatly dependent on the hydrogenation catalyzed by the noble metals, which is a cost-intensive and energy-intensive process [85]. Therefore, the development of new materials for energy-efficient separation by adsorption is designed in order to perform the removal of propylene from the propylene/propylene mixture [86].

In this work, three gallate-based MOFs, M-gallate (M(C<sub>7</sub>O<sub>5</sub>H<sub>4</sub>)·2H<sub>2</sub>O, M = Co, Ni, Mg) with high chemical stability, and three-dimensionally interconnected zigzag channels are investigated. The minimum aperture sizes of the studied materials are 3.69, 3.56 and 3.47 Å for Co-gallate, Mg-gallate and Ni-gallate, respectively. All the three gallate materials displayed high propylene uptake at 298 K and 1 bar conditions. Mg-gallate showed the highest propylene uptake, which was 3.75 mmol/g, followed by Co-gallate and Ni-gallate with 3.21 and 2.65 mmol/g, respectively. The low affinity between propylene with the frameworks is observed by the low propylene uptake of 1.50, 1.49 and 0.90 mmol/g for Mg-gallate, Co-gallate and Ni-gallate, respectively. These porous materials also demonstrated a remarkable separation performance by presenting the high IAST selectivity at ambient conditions, which were 152, 113 and 65 for Co-gallate, Ni-gallate and Mg-gallate, respectively.

The isosteric enthalpy of adsorption ( $Q_{st}$ ) is presented in order to evaluate the strong interactions between propylene molecules and the frameworks. The values of  $Q_{st}$  of propylene molecules are 84, 82 and 66 kJ/mol for Ni-gallate, Co-gallate and Mg-gallate, respectively. In contrast, the values of  $Q_{st}$  of propylene molecules for Ni-gallate, Co-gallate and Mg-gallate are 53, 47 and 44 kJ/mol, respectively. This significant difference of  $Q_{st}$  between propyne and propylene molecules showed that gallate-based MOFs are promising materials for the efficient capture of propylene trace in the propylene product



line. Therefore, this work demonstrated an alternative method of purifying propylene through an energy-efficient technology.

### 3.5. Summary of the Applications of Gallate-Based MOFs

Table 1 shows the summary of studies on gallate-based MOFs conducted by the previous works.

**Table 1.** Previous studies on gallate-based MOFs.

M-Gallate	Application	References
M = Fe(III)	Iron gall ink	[57]
M = La(III), Nd(III), Pr(III)	Superconductors	[58]
M = Fe(III), Mn(II), Co(II), Ni(II)	Magnetic materials.	[33,40]
Biomedical applications:		
M = Mg(II), Ca(II)	(i) Antioxidant carrier	[61,62]
M = Cu(II)	(ii) Anticancer agent	[64]
Hydrocarbon separations:		
M = Ni(II), Mg(II), Co(II)	(i) Adsorptive separation of ethylene from ethylene/ethane mixture.	[35]
	(ii) Adsorptive separation of acetylene from acetylene/ethylene mixture.	[54]
	(iii) Adsorptive separation of <i>trans/cis</i> -2-butene.	[83]
	(iv) Adsorptive separation of propylene from propylene/propylene mixture.	[86]

It can be concluded that the applications of gallate-based MOFs in industry are still limited. Mostly, gallate-based MOFs have been used in biomedical applications and are gradually showing remarkable performance as the new alternative materials in chemical industrial applications, especially when they are first reported for the adsorptive separation of light hydrocarbon separations. The pore aperture sizes of gallate-based MOFs played an important role in cost and energy-efficient adsorption by allowing the smaller molecules to pass through and be captured in the pore channel, while prohibiting the larger molecules from entering the pore. These porous materials have a bright future and can be kept in development for various applications in order to be applied in real industrial practices. Nevertheless, the real industrial practices of these have fallen far behind academic research. For that reason, research into the practicability of synthesizing and applying MOFs for potential industrial applications is of great interest.

## 4. Future Potential Application of Gallate-Based MOFs

Many of the studies have emphasized the utilization of MOFs in the adsorption process as a way of storing fuel gases such as hydrogen (H<sub>2</sub>) and methane (CH<sub>4</sub>) [87], as well as carbon dioxide (CO<sub>2</sub>) [88]. Until now, MOFs have been studied for the gas storage of H<sub>2</sub>, CH<sub>4</sub> and CO<sub>2</sub>, among other gases [89]. Meanwhile, there are also many MOFs that can illustrate high adsorption selectivity in CO<sub>2</sub>/CH<sub>4</sub>, CO<sub>2</sub>/N<sub>2</sub>, CO<sub>2</sub>/H<sub>2</sub> and CH<sub>4</sub>/H<sub>2</sub> separations, because MOFs can be designed to create stronger adsorption sites for gas molecules and as a result the gas selectivity of materials can be increased [90]. The gas capture, gas storage, gas purification and gas separation applications which involved the new family gallate-based MOFs are very limited to date, since only light hydrocarbon separations have been reported before, and none of them are related to CO<sub>2</sub>/CH<sub>4</sub> separations. Therefore, this circumstance creates a new opportunity to concentrate more on studies of gallate-based MOFs in CO<sub>2</sub>/CH<sub>4</sub> applications.

Carbon dioxide capture and separation can be divided into three main types of applications in industry, which are postcombustion capture and separation, precombustion capture and separation,

and the purification of natural gas [91]. Natural gas processing is considered to be the largest industrial gas separation application, since it involves more than USD 5 billion annually for the worldwide market of natural gas separation equipment [92]. The removal of CO<sub>2</sub> is necessary, as it can reduce the energy content of natural gas and is also corrosive in the presence of water, which can cause several problems related to pipelines transport [93].

There are about 83 trillion ft<sup>3</sup> of natural gas reservoirs which contain 28–87% of the CO<sub>2</sub> content in Malaysia [94]. Because of the CO<sub>2</sub> content, it is stated that over 13 trillion ft<sup>3</sup> of the natural gas reservoirs remain unexploited [95]. Since there are limited natural gas reservoirs with low CO<sub>2</sub> content, the exploitation of these high CO<sub>2</sub> content natural gas fields is required so that Malaysia can increase its natural gas production extensively in order to meet the high worldwide energy demands [94]. The discovery of natural gas fields with high CO<sub>2</sub> content up to 87% in Malaysia created new challenges with respect to the CO<sub>2</sub> separation process. High CO<sub>2</sub> gas fields in Malaysia are considered as unconventional gas fields, since the gas has a low heating value. Furthermore, high CO<sub>2</sub> content is also subject to the hydrate formation threat [96]. Therefore, the gas needs to be processed to make it a valuable and marketable product. High CO<sub>2</sub> content gas fields made most of the gas field development uneconomical, and it has remained undeveloped as it required the careful management of CO<sub>2</sub> capture, transportation, storage and utilization to enable the commercialization of these gas fields [97]. High CO<sub>2</sub> gas fields in Malaysia have represented an excellent opportunity for significant CO<sub>2</sub> capture and storage (CCS) [97].

The pore sizes and shapes of MOFs can be efficiently varied by the choice of the metal secondary building units and organic linker [91]. One of the strategies to improve the capture and selectivity of CO<sub>2</sub> over CH<sub>4</sub> is to enhance the pore size and shape in order to regulate the interactions between pore surface and CO<sub>2</sub> molecules [91]. Based on the previous work, the aperture sizes of gallate-based MOFs are within the range of 3.47 Å to 3.69 Å [54]. Meanwhile, the kinetics diameter of CO<sub>2</sub> and CH<sub>4</sub> is 3.3 Å and 3.8 Å, respectively [98]. Theoretically, this fact will explain why gallate-based MOFs can selectively capture CO<sub>2</sub> from CO<sub>2</sub>/CH<sub>4</sub> mixture based on the size differentiation, and, therefore, have a promising future as adsorbent materials in CO<sub>2</sub>/CH<sub>4</sub> separation. Figure 5 shows the schematic diagram of the size-selective separation of CO<sub>2</sub> and CH<sub>4</sub>.

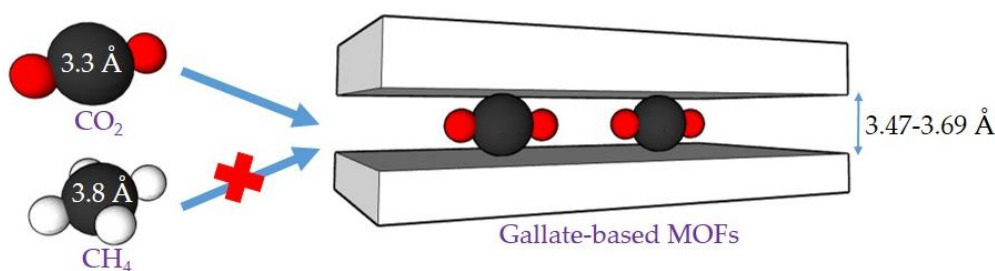


**Figure 5.** Schematic diagram of size-selective separation of CO<sub>2</sub> and CH<sub>4</sub>.

In addition, CO<sub>2</sub> has a larger polarizability ( $29.1 \times 10^{-25} \text{ cm}^3$  for CO<sub>2</sub>,  $25.9 \times 10^{-25} \text{ cm}^3$  for CH<sub>4</sub>) and quadrupole moment ( $4.30 \times 10^{-26} \text{ esu cm}^2$  for CO<sub>2</sub>, 0 for CH<sub>4</sub>) compared to CH<sub>4</sub>, which led to a stronger interaction between CO<sub>2</sub> and MOFs [81]. Since the intrinsic quadrupole moment of the CO<sub>2</sub> molecule exists, it is possible to enrich CO<sub>2</sub> uptake by introducing a polar functional group in the framework of porous materials [99]. Gallic acid which is comprised of three hydroxyl groups has an advantage, because MOFs with a polar functional group preferred the CO<sub>2</sub> adsorption over methane with remarkable selectivity [98]. This is due to the polar functional groups which have stronger adsorbate–adsorbent interactions for CO<sub>2</sub> that can increase both capacity and selectivity [100]. On top of that, gallic acid itself is a polar compound [101]. In addition, carbonyl functional group and hydroxyl functional groups in gallic acid are also suitable for gas adsorption, specifically for CO<sub>2</sub> capture [102]. Indeed, the introduction of organic linker with certain functional groups into the framework should enhance the host–guest interactions between MOFs and guest molecules [102].

Therefore, gallate-based MOFs are among the new promising candidates in natural gas separations, especially for CO<sub>2</sub>/CH<sub>4</sub> mixtures.

## 5. Conclusions

Gallic acid as an organic linker gave a new concept in forming MOFs known as gallate-based MOFs from a lower-cost and lower-toxicity material. Based on the previous studies, it can be shown that gallate-based MOFs are relevant to chemical industrial applications, despite only being emphasized in biomedical areas. Theoretically, gallate-based MOFs, which can act as potential adsorbents, can attract a great deal of interest to sustain the economic and environmentally friendly CO<sub>2</sub> adsorption processes. In addition, gallate-based MOFs can also lead to the commercialization of newly designed CO<sub>2</sub> adsorbents, in which the exploitation of high CO<sub>2</sub> content reservoirs and other CO<sub>2</sub> removal applications can be solved.

**Author Contributions:** Writing—original draft preparation, M.I.; Conceptualization, M.A.B.; Writing—review and editing, M.I. and M.A.B.; Supervision, M.A.B. and Y.F.Y.; Project administration, M.A.B.; Funding acquisition, M.A.B. All authors have read and agreed to the published version of the manuscript.

**Funding:** This research was funded by Yayasan Universiti Teknologi PETRONAS (YUTP), grant no 0153AA-H42 and Graduate Assistantship Scheme by Universiti Teknologi PETRONAS.

**Acknowledgments:** This research was supported by Carbon Dioxide Research Centre (CO<sub>2</sub>RES), Universiti Teknologi PETRONAS.

**Conflicts of Interest:** The authors declare there is no conflict of interest.

## References

1. Choi, I.; Jung, Y.E.; Yoo, S.J.; Kim, J.Y.; Kim, H.-J.; Lee, C.Y.; Jang, J.H. Facile Synthesis of M-MOF-74 (M = Co, Ni, Zn) and its Application as an ElectroCatalyst for Electrochemical CO<sub>2</sub> Conversion and H<sub>2</sub> Production. *J. Electrochem. Sci. Technol.* **2017**, *8*, 61–68. [[CrossRef](#)]
2. Yuan, D.; Zhao, D.; Sun, D.; Zhou, H.C. An isoreticular series of metal–organic frameworks with dendritic hexacarboxylate ligands and exceptionally high gas-uptake capacity. *Angew. Chem. Int. Ed.* **2010**, *49*, 5357–5361. [[CrossRef](#)] [[PubMed](#)]
3. Keskin, S.; Kizilel, S. Biomedical applications of metal organic frameworks. *Ind. Eng. Chem. Res.* **2011**, *50*, 1799–1812. [[CrossRef](#)]
4. Li, J.-R.; Ma, Y.; McCarthy, M.C.; Sculley, J.; Yu, J.; Jeong, H.-K.; Balbuena, P.B.; Zhou, H.-C. Carbon dioxide capture-related gas adsorption and separation in metal-organic frameworks. *Coord. Chem. Rev.* **2011**, *255*, 1791–1823. [[CrossRef](#)]
5. Yaghi, O.; Li, G. Mutually interpenetrating sheets and channels in the extended structure of [Cu(4,4'-bpy)Cl]. *Angew. Chem. Int. Ed. Engl.* **1995**, *34*, 207–209. [[CrossRef](#)]
6. Rosi, N.L.; Kim, J.; Eddaoudi, M.; Chen, B.; O’Keeffe, M.; Yaghi, O.M. Rod packings and metal–organic frameworks constructed from rod-shaped secondary building units. *J. Am. Chem. Soc.* **2005**, *127*, 1504–1518. [[CrossRef](#)]
7. Ullah, S.; Bustam, M.A.; Assiri, M.A.; Al-Sehemi, A.G.; Sagir, M.; Abdul Kareem, F.A.; Elkhalfah, A.E.I.; Mukhtar, A.; Gonfa, G. Synthesis, and characterization of metal-organic frameworks-177 for static and dynamic adsorption behavior of CO<sub>2</sub> and CH<sub>4</sub>. *Microporous Mesoporous Mater.* **2019**, *288*, 109569. [[CrossRef](#)]
8. Kaye, S.S.; Dailly, A.; Yaghi, O.M.; Long, J.R. Impact of preparation and handling on the hydrogen storage properties of Zn<sub>4</sub>O(1,4-benzenedicarboxylate)<sub>3</sub>(MOF-5). *J. Am. Chem. Soc.* **2007**, *129*, 14176–14177. [[CrossRef](#)]
9. Park, K.S.; Ni, Z.; Côté, A.P.; Choi, J.Y.; Huang, R.; Uribe-Romo, F.J.; Chae, H.K.; O’Keeffe, M.; Yaghi, O.M. Exceptional chemical and thermal stability of zeolitic imidazolate frameworks. *Proc. Natl. Acad. Sci. USA* **2006**, *103*, 10186–10191. [[CrossRef](#)]
10. Raganati, F.; Gargiulo, V.; Ammendola, P.; Alfe, M.; Chirone, R. CO<sub>2</sub> capture performance of HKUST-1 in a sound assisted fluidized bed. *Chem. Eng. J.* **2014**, *239*, 75–86. [[CrossRef](#)]
11. Férey, G.; Mellot-Draznieks, C.; Serre, C.; Millange, F.; Dutour, J.; Surblé, S.; Margiolaki, I. A chromium terephthalate-based solid with unusually large pore volumes and surface area. *Science* **2005**, *309*, 2040–2042. [[CrossRef](#)] [[PubMed](#)]

12. Walton, K.S.; Millward, A.R.; Dubbeldam, D.; Frost, H.; Low, J.J.; Yaghi, O.M.; Snurr, R.Q. Understanding inflections and steps in carbon dioxide adsorption isotherms in metal-organic frameworks. *J. Am. Chem. Soc.* **2008**, *130*, 406–407. [[CrossRef](#)]
13. Cavka, J.H.; Jakobsen, S.; Olsbye, U.; Guillou, N.; Lamberti, C.; Bordiga, S.; Lillerud, K.P. A new zirconium inorganic building brick forming metal organic frameworks with exceptional stability. *J. Am. Chem. Soc.* **2008**, *130*, 13850–13851. [[CrossRef](#)] [[PubMed](#)]
14. Mondloch, J.E.; Bury, W.; Fairen-Jimenez, D.; Kwon, S.; DeMarco, E.J.; Weston, M.H.; Sarjeant, A.A.; Nguyen, S.T.; Stair, P.C.; Snurr, R.Q. Vapor-phase metalation by atomic layer deposition in a metal-organic framework. *J. Am. Chem. Soc.* **2013**, *135*, 10294–10297. [[CrossRef](#)] [[PubMed](#)]
15. Biswas, S.; Grzywa, M.; Nayek, H.P.; Dehnen, S.; Senkovska, I.; Kaskel, S.; Volkmer, D. A cubic coordination framework constructed from benzobistriazolate ligands and zinc ions having selective gas sorption properties. *Dalton Trans.* **2009**, 6487–6495. [[CrossRef](#)] [[PubMed](#)]
16. Yang, S.; Ramirez-Cuesta, A.J.; Newby, R.; Garcia-Sakai, V.; Manuel, P.; Callear, S.K.; Campbell, S.I.; Tang, C.C.; Schröder, M. Supramolecular binding and separation of hydrocarbons within a functionalized porous metal-organic framework. *Nat. Chem.* **2015**, *7*, 121. [[CrossRef](#)] [[PubMed](#)]
17. Kamal, K.; Bustam, M.A.; Ismail, M.; Grekov, D.; Mohd Shariff, A.; Pré, P. Optimization of Washing Processes in Solvothermal Synthesis of Nickel-Based MOF-74. *Materials* **2020**, *13*, 2741. [[CrossRef](#)] [[PubMed](#)]
18. Cho, H.-Y.; Yang, D.-A.; Kim, J.; Jeong, S.-Y.; Ahn, W.-S. CO<sub>2</sub> adsorption and catalytic application of Co-MOF-74 synthesized by microwave heating. *Catal. Today* **2012**, *185*, 35–40. [[CrossRef](#)]
19. Niu, H.; Zheng, Y.; Wang, S.; He, S.; Cai, Y. Stable hierarchical microspheres of 1D Fe-gallic acid MOFs for fast and efficient Cr (VI) elimination by a combination of reduction, metal substitution and coprecipitation. *J. Mater. Chem. A* **2017**, *5*, 16600–16604. [[CrossRef](#)]
20. Krishna, R.; Long, J.R. Screening metal-organic frameworks by analysis of transient breakthrough of gas mixtures in a fixed bed adsorber. *J. Phys. Chem. C* **2011**, *115*, 12941–12950. [[CrossRef](#)]
21. Matsuda, R. Design and synthesis of porous coordination polymers showing unique guest adsorption behaviors. *Bull. Chem. Soc. Jpn.* **2013**, *86*, 1117–1131. [[CrossRef](#)]
22. Getman, R.B.; Bae, Y.-S.; Wilmer, C.E.; Snurr, R.Q. Review and analysis of molecular simulations of methane, hydrogen, and acetylene storage in metal-organic frameworks. *Chem. Rev.* **2012**, *112*, 703–723. [[CrossRef](#)] [[PubMed](#)]
23. Sun, C.-Y.; Qin, C.; Wang, X.-L.; Su, Z.-M. Metal-organic frameworks as potential drug delivery systems. *Expert Opin. Drug Deliv.* **2013**, *10*, 89–101. [[CrossRef](#)] [[PubMed](#)]
24. Gu, Z.Y.; Park, J.; Raiff, A.; Wei, Z.; Zhou, H.C. Metal-organic frameworks as biomimetic catalysts. *ChemCatChem* **2014**, *6*, 67–75. [[CrossRef](#)]
25. Tian, Y.; Cong, J.; Shen, S.; Chai, Y.; Yan, L.; Wang, S.; Sun, Y. Electric control of magnetism in a multiferroic metal-organic framework. *Phys. Status Solidi (RRL)–Rapid Res. Lett.* **2014**, *8*, 91–94. [[CrossRef](#)]
26. Cui, Y.; Yue, Y.; Qian, G.; Chen, B. Luminescent functional metal-organic frameworks. *Chem. Rev.* **2012**, *112*, 1126–1162. [[CrossRef](#)]
27. Kreno, L.E.; Leong, K.; Farha, O.K.; Allendorf, M.; Van Duyne, R.P.; Hupp, J.T. Metal-organic framework materials as chemical sensors. *Chem. Rev.* **2012**, *112*, 1105–1125. [[CrossRef](#)]
28. Demir, S.; Çepni, H.M.; Topcu, Y.; Hołyńska, M.; Keskin, S. A phytochemical-containing metal-organic framework: Synthesis, characterization and molecular simulations for hydrogen adsorption. *Inorg. Chim. Acta* **2015**, *427*, 138–143. [[CrossRef](#)]
29. Hu, Z.; Wang, Y.; Shah, B.B.; Zhao, D. CO<sub>2</sub> Capture in Metal-Organic Framework Adsorbents: An Engineering Perspective. *Adv. Sustain. Syst.* **2019**, *3*, 1800080. [[CrossRef](#)]
30. Silva, P.; Vilela, S.M.; Tomé, J.P.; Paz, F.A.A. Multifunctional metal-organic frameworks: From academia to industrial applications. *Chem. Soc. Rev.* **2015**, *44*, 6774–6803. [[CrossRef](#)]
31. DeSantis, D.; Mason, J.A.; James, B.D.; Houchins, C.; Long, J.R.; Veenstra, M. Techno-economic analysis of metal-organic frameworks for hydrogen and natural gas storage. *Energy Fuels* **2017**, *31*, 2024–2032. [[CrossRef](#)]
32. Nyamai, D.W.; Arika, W.; Ogola, P.; Njagi, E.; Ngugi, M. Medicinally important phytochemicals: An untapped research avenue. *J. Pharmacogn. Phytochem.* **2016**, *4*, 35–49.

33. Saines, P.J.; Yeung, H.H.-M.; Hester, J.R.; Lennie, A.R.; Cheetham, A.K. Detailed investigations of phase transitions and magnetic structure in Fe(III), Mn(II), Co(II) and Ni(II) 3,4,5-trihydroxybenzoate (gallate) dihydrates by neutron and X-ray diffraction. *Dalton Trans.* **2011**, *40*, 6401–6410. [[CrossRef](#)] [[PubMed](#)]
34. Li, L.; Lin, R.-B.; Krishna, R.; Wang, X.; Li, B.; Wu, H.; Li, J.; Zhou, W.; Chen, B. Flexible–robust metal–organic framework for efficient removal of propyne from propylene. *J. Am. Chem. Soc.* **2017**, *139*, 7733–7736. [[CrossRef](#)] [[PubMed](#)]
35. Bao, Z.; Wang, J.; Zhang, Z.; Xing, H.; Yang, Q.; Yang, Y.; Wu, H.; Krishna, R.; Zhou, W.; Chen, B. Molecular Sieving of Ethane from Ethylene through the Molecular Cross-Section Size Differentiation in Gallate-based Metal–Organic Frameworks. *Angew. Chem.* **2018**, *130*, 16252–16257. [[CrossRef](#)]
36. Nayeem, N.; Asdaq, S.; Salem, H.; AHEI-Alfgy, S. Gallic acid: A promising lead molecule for drug development. *J. Appl. Pharm.* **2016**, *8*, 1–4. [[CrossRef](#)]
37. Marino, T.; Galano, A.; Russo, N. Radical scavenging ability of gallic acid toward OH and OOH radicals. Reaction mechanism and rate constants from the density functional theory. *J. Phys. Chem. B* **2014**, *118*, 10380–10389. [[CrossRef](#)] [[PubMed](#)]
38. Badhani, B.; Sharma, N.; Kakkar, R. Gallic acid: A versatile antioxidant with promising therapeutic and industrial applications. *RSC Adv.* **2015**, *5*, 27540–27557. [[CrossRef](#)]
39. Galanakis, C.; Goulas, V.; Tsakona, S.; Manganaris, G.; Gekas, V. A knowledge base for the recovery of natural phenols with different solvents. *Int. J. Food Prop.* **2013**, *16*, 382–396. [[CrossRef](#)]
40. Feller, R.K.; Cheetham, A.K. Fe(III), Mn(II), Co(II), and Ni(II) 3,4,5-trihydroxybenzoate (gallate) dihydrates; a new family of hybrid framework materials. *Solid State Sci.* **2006**, *8*, 1121–1125. [[CrossRef](#)]
41. El Gharras, H. Polyphenols: Food sources, properties and applications—a review. *Int. J. Food Sci. Technol.* **2009**, *44*, 2512–2518. [[CrossRef](#)]
42. Cheynier, V. Polyphenols in foods are more complex than often thought. *Am. J. Clin. Nutr.* **2005**, *81*, 223S–229S. [[CrossRef](#)]
43. Fernandes, F.H.A.; Salgado, H.R.N. Gallic acid: Review of the methods of determination and quantification. *Crit. Rev. Anal. Chem.* **2016**, *46*, 257–265. [[CrossRef](#)]
44. Daneshfar, A.; Ghaziaskar, H.S.; Homayoun, N. Solubility of gallic acid in methanol, ethanol, water, and ethyl acetate. *J. Chem. Eng. Data* **2008**, *53*, 776–778. [[CrossRef](#)]
45. Kim, S.-H.; Jun, C.-D.; Suk, K.; Choi, B.-J.; Lim, H.; Park, S.; Lee, S.H.; Shin, H.-Y.; Kim, D.-K.; Shin, T.-Y. Gallic acid inhibits histamine release and pro-inflammatory cytokine production in mast cells. *Toxicol. Sci.* **2006**, *91*, 123–131. [[CrossRef](#)] [[PubMed](#)]
46. Kroes, B.V.; Van den Berg, A.; Van Ufford, H.Q.; Van Dijk, H.; Labadie, R. Anti-inflammatory activity of gallic acid. *Planta Med.* **1992**, *58*, 499–504. [[CrossRef](#)] [[PubMed](#)]
47. Choi, H.J.; Song, J.H.; Bhatt, L.R.; Baek, S.H. Anti-human rhinovirus activity of gallic acid possessing antioxidant capacity. *Phytother. Res.* **2010**, *24*, 1292–1296. [[CrossRef](#)] [[PubMed](#)]
48. Kubo, I.; Xiao, P.; Fujita, K.I. Antifungal activity of octyl gallate: Structural criteria and mode of action. *Bioorg. Med. Chem. Lett.* **2001**, *11*, 347–350. [[CrossRef](#)]
49. Abdelwahed, A.; Bouhleb, I.; Skandrani, I.; Valenti, K.; Kadri, M.; Guiraud, P.; Steiman, R.; Mariotte, A.-M.; Ghedira, K.; Laporte, F. Study of antimutagenic and antioxidant activities of Gallic acid and 1, 2, 3, 4, 6-pentagalloylglucose from Pistacia lentiscus: Confirmation by microarray expression profiling. *Chem. Biol. Interact.* **2007**, *165*, 1–13. [[CrossRef](#)]
50. Priscilla, D.H.; Prince, P.S.M. Cardioprotective effect of gallic acid on cardiac troponin-T, cardiac marker enzymes, lipid peroxidation products and antioxidants in experimentally induced myocardial infarction in Wistar rats. *Chem. Biol. Interact.* **2009**, *179*, 118–124. [[CrossRef](#)]
51. Lu, Z.; Nie, G.; Belton, P.S.; Tang, H.; Zhao, B. Structure–activity relationship analysis of antioxidant ability and neuroprotective effect of gallic acid derivatives. *Neurochem. Int.* **2006**, *48*, 263–274. [[CrossRef](#)]
52. Giftson, J.S.; Jayanthi, S.; Nalini, N. Chemopreventive efficacy of gallic acid, an antioxidant and anticarcinogenic polyphenol, against 1,2-dimethyl hydrazine induced rat colon carcinogenesis. *Investig. New Drugs* **2010**, *28*, 251–259. [[CrossRef](#)] [[PubMed](#)]
53. Zhu, J.; Chen, F.; Zhang, Z.; Li, M.; Yang, Q.; Yang, Y.; Bao, Z.; Ren, Q. M-Gallate (M= Ni, Co) Metal–Organic Framework-Derived Ni/C and Bimetallic Ni–Co/C Catalysts for Lignin Conversion into Monophenols. *ACS Sustain. Chem. Eng.* **2019**, *7*, 12955–12963. [[CrossRef](#)]

54. Wang, J.; Li, L.; Guo, L.; Zhao, Y.; Xie, D.; Zhang, Z.; Yang, Q.; Yang, Y.; Bao, Z.; Ren, Q. Adsorptive separation of acetylene from ethylene in isostructural gallate-based metal-organic frameworks. *Chem. A Eur. J.* **2019**, *25*, 15516–15524. [[CrossRef](#)]
55. Henniges, U.; Banik, G.; Reibke, R.; Potthast, A. Studies into the early degradation stages of cellulose by different iron gall ink components. *Macromol. Symp.* **2008**, *262*, 150–161. [[CrossRef](#)]
56. Wunderlich, C.H.; Weber, R.; Bergerhoff, G. Über Eisengallustinte. *Z. Für Anorg. Allg. Chem.* **1991**, *598*, 371–376. [[CrossRef](#)]
57. Ponce, A.; Brostoff, L.B.; Gibbons, S.K.; Zavalij, P.; Viragh, C.; Hooper, J.; Alnemrat, S.; Gaskell, K.J.; Eichhorn, B. Elucidation of the Fe(III) gallate structure in historical iron gall ink. *Anal. Chem.* **2016**, *88*, 5152–5158. [[CrossRef](#)] [[PubMed](#)]
58. Berkstresser, G.; Valentino, A.; Brandle, C. Growth of single crystals of rare earth gallates. *J. Cryst. Growth* **1991**, *109*, 457–466. [[CrossRef](#)]
59. Chedid, G.; Yassin, A. Recent trends in covalent and metal organic frameworks for biomedical applications. *Nanomaterials* **2018**, *8*, 916. [[CrossRef](#)] [[PubMed](#)]
60. Horcajada, P.; Serre, C.; McKinlay, A.C.; Morris, R.E. Biomedical applications of metal-organic frameworks. *Met. Org. Framew. Appl. Catal. Gas Storage* **2011**, 213–250.
61. Cooper, L.; Hidalgo, T.; Gorman, M.; Lozano-Fernández, T.; Simón-Vázquez, R.; Olivier, C.; Guillou, N.; Serre, C.; Martineau, C.; Taulelle, F. A biocompatible porous Mg-gallate metal-organic framework as an antioxidant carrier. *Chem. Commun.* **2015**, *51*, 5848–5851. [[CrossRef](#)] [[PubMed](#)]
62. Hidalgo, T.; Cooper, L.; Gorman, M.; Lozano-Fernández, T.; Simón-Vázquez, R.; Mouchaham, G.; Marrot, J.; Guillou, N.; Serre, C.; Fertey, P. Crystal structure dependent in vitro antioxidant activity of biocompatible calcium gallate MOFs. *J. Mater. Chem. B* **2017**, *5*, 2813–2822. [[CrossRef](#)] [[PubMed](#)]
63. Cai, W.; Chu, C.C.; Liu, G.; Wang, Y.X.J. Metal-organic framework-based nanomedicine platforms for drug delivery and molecular imaging. *Small* **2015**, *11*, 4806–4822. [[CrossRef](#)] [[PubMed](#)]
64. Sharma, S.; Mittal, D.; Verma, A.K.; Roy, I. Copper-Gallic Acid Nanoscale Metal-Organic Framework for Combined Drug Delivery and Photodynamic Therapy. *ACS Appl. Bio Mater.* **2019**, *2*, 2092–2101. [[CrossRef](#)]
65. Kang, Z.; Fan, L.; Sun, D. Recent advances and challenges of metal-organic framework membranes for gas separation. *J. Mater. Chem. A* **2017**, *5*, 10073–10091. [[CrossRef](#)]
66. Bao, Z.; Chang, G.; Xing, H.; Krishna, R.; Ren, Q.; Chen, B. Potential of microporous metal-organic frameworks for separation of hydrocarbon mixtures. *Energy Environ. Sci.* **2016**, *9*, 3612–3641. [[CrossRef](#)]
67. Czaja, A.U.; Trukhan, N.; Müller, U. Industrial applications of metal-organic frameworks. *Chem. Soc. Rev.* **2009**, *38*, 1284–1293. [[CrossRef](#)]
68. Yilmaz, B.; Trukhan, N.; Müller, U. Industrial outlook on zeolites and metal organic frameworks. *Chin. J. Catal.* **2012**, *33*, 3–10. [[CrossRef](#)]
69. Valizadeh, B.; Nguyen, T.N.; Stylianou, K.C. Shape engineering of metal-organic frameworks. *Polyhedron* **2018**, *145*, 1–15. [[CrossRef](#)]
70. Kalmutzki, M.J.; Hanikel, N.; Yaghi, O.M. Secondary building units as the turning point in the development of the reticular chemistry of MOFs. *Sci. Adv.* **2018**, *4*, eaat9180. [[CrossRef](#)]
71. Hong, X.-J.; Wei, Q.; Cai, Y.-P.; Wu, B.-b.; Feng, H.-X.; Yu, Y.; Dong, R.-F. Pillar-layered metal-organic framework with sieving effect and pore space partition for effective separation of mixed gas C<sub>2</sub>H<sub>2</sub>/C<sub>2</sub>H<sub>4</sub>. *ACS Appl. Mater. Interfaces* **2017**, *9*, 29374–29379. [[CrossRef](#)]
72. Lin, R.-B.; Li, L.; Zhou, H.-L.; Wu, H.; He, C.; Li, S.; Krishna, R.; Li, J.; Zhou, W.; Chen, B. Molecular sieving of ethylene from ethane using a rigid metal-organic framework. *Nat. Mater.* **2018**, *17*, 1128–1133. [[CrossRef](#)] [[PubMed](#)]
73. Kim, A.-R.; Yoon, T.-U.; Kim, E.-J.; Yoon, J.W.; Kim, S.-Y.; Yoon, J.W.; Hwang, Y.K.; Chang, J.-S.; Bae, Y.-S. Facile loading of Cu(I) in MIL-100 (Fe) through redox-active Fe(II) sites and remarkable propylene/propane separation performance. *Chem. Eng. J.* **2018**, *331*, 777–784. [[CrossRef](#)]
74. Ye, Y.; Ma, Z.; Lin, R.-B.; Krishna, R.; Zhou, W.; Lin, Q.; Zhang, Z.; Xiang, S.; Chen, B. Pore space partition within a metal-organic framework for highly efficient C<sub>2</sub>H<sub>2</sub>/CO<sub>2</sub> separation. *J. Am. Chem. Soc.* **2019**, *141*, 4130–4136. [[CrossRef](#)] [[PubMed](#)]
75. Furukawa, H.; Cordova, K.E.; O’Keeffe, M.; Yaghi, O.M. The chemistry and applications of metal-organic frameworks. *Science* **2013**, *341*, 1230444. [[CrossRef](#)] [[PubMed](#)]

76. Lin, R.-B.; Xiang, S.; Xing, H.; Zhou, W.; Chen, B. Exploration of porous metal–organic frameworks for gas separation and purification. *Coord. Chem. Rev.* **2019**, *378*, 87–103. [[CrossRef](#)]
77. Gao, F.; Wang, Y.; Wang, X.; Wang, S. Adsorptive separation of ethylene/ethane mixtures with CuCl@ HY adsorbent: Equilibrium and reversibility. *J. Porous Mater.* **2017**, *24*, 713–719. [[CrossRef](#)]
78. Moura, L.; Darwich, W.; Santini, C.C.; Gomes, M.F.C. Imidazolium-based ionic liquids with cyano groups for the selective absorption of ethane and ethylene. *Chem. Eng. J.* **2015**, *280*, 755–762. [[CrossRef](#)]
79. Wen, H.-M.; Li, B.; Wang, H.; Krishna, R.; Chen, B. High acetylene/ethylene separation in a microporous zinc (II) metal–organic framework with low binding energy. *Chem. Commun.* **2016**, *52*, 1166–1169. [[CrossRef](#)]
80. Hazra, A.; Jana, S.; Bonakala, S.; Balasubramanian, S.; Maji, T.K. Separation/purification of ethylene from an acetylene/ethylene mixture in a pillared-layer porous metal–organic framework. *Chem. Commun.* **2017**, *53*, 4907–4910. [[CrossRef](#)]
81. Cui, W.G.; Hu, T.L.; Bu, X.H. Metal–Organic Framework Materials for the Separation and Purification of Light Hydrocarbons. *Adv. Mater.* **2019**, *32*, 1806445. [[CrossRef](#)] [[PubMed](#)]
82. Kishida, K.; Okumura, Y.; Watanabe, Y.; Mukoyoshi, M.; Bracco, S.; Comotti, A.; Sozzani, P.; Horike, S.; Kitagawa, S. Recognition of 1,3-Butadiene by a Porous Coordination Polymer. *Angew. Chem. Int. Ed.* **2016**, *55*, 13784–13788. [[CrossRef](#)]
83. Chen, J.; Wang, J.; Guo, L.; Li, L.; Yang, Q.; Zhang, Z.; Yang, Y.; Bao, Z.; Ren, Q. Adsorptive Separation of Geometric Isomers of 2-Butene on Gallate-Based Metal-Organic Frameworks. *ACS Appl. Mater. Interfaces* **2020**, *12*, 9609–9616. [[CrossRef](#)] [[PubMed](#)]
84. Cadiou, A.; Adil, K.; Bhatt, P.; Belmabkhout, Y.; Eddaoudi, M. A metal-organic framework–based splitter for separating propylene from propane. *Science* **2016**, *353*, 137–140. [[CrossRef](#)]
85. Yang, L.; Cui, X.; Yang, Q.; Qian, S.; Wu, H.; Bao, Z.; Zhang, Z.; Ren, Q.; Zhou, W.; Chen, B. A Single-Molecule Propyne Trap: Highly Efficient Removal of Propyne from Propylene with Anion-Pillared Ultramicroporous Materials. *Adv. Mater.* **2018**, *30*, 1705374. [[CrossRef](#)]
86. Li, Z.; Li, L.; Guo, L.; Wang, J.; Yang, Q.; Zhang, Z.; Yang, Y.; Bao, Z.; Ren, Q. Gallate-Based Metal-Organic Frameworks for Highly Efficient Removal of Trace Propyne from Propylene. *Ind. Eng. Chem. Res.* **2020**, *59*, 13716–13723. [[CrossRef](#)]
87. Glover, T.G.; Peterson, G.W.; Schindler, B.J.; Britt, D.; Yaghi, O. MOF-74 building unit has a direct impact on toxic gas adsorption. *Chem. Eng. Sci.* **2011**, *66*, 163–170. [[CrossRef](#)]
88. Sumida, K.; Rogow, D.L.; Mason, J.A.; McDonald, T.M.; Bloch, E.D.; Herm, Z.R.; Bae, T.-H.; Long, J.R. Carbon dioxide capture in metal–organic frameworks. *Chem. Rev.* **2011**, *112*, 724–781. [[CrossRef](#)] [[PubMed](#)]
89. Wang, B.; Zhang, X.; Huang, H.; Zhang, Z.; Yildirim, T.; Zhou, W.; Xiang, S.; Chen, B. A microporous aluminum-based metal-organic framework for high methane, hydrogen, and carbon dioxide storage. *Nano Res.* **2020**, *1–5*. [[CrossRef](#)]
90. Sezginel, K.B.; Keskin, S.; Uzun, A. Tuning the gas separation performance of CuBTC by ionic liquid incorporation. *Langmuir* **2016**, *32*, 1139–1147. [[CrossRef](#)]
91. Li, B.; Wang, H.; Chen, B. Microporous metal–organic frameworks for gas separation. *Chem. Asian J.* **2014**, *9*, 1474–1498. [[CrossRef](#)]
92. Esmaeili, A. Supersonic separation of natural gas liquids by Twister technology. *Chem. Eng. Trans.* **2016**, *52*, 7–12.
93. Keskin, S.; Sholl, D.S. Selecting metal organic frameworks as enabling materials in mixed matrix membranes for high efficiency natural gas purification. *Energy Environ. Sci.* **2010**, *3*, 343–351. [[CrossRef](#)]
94. Ghazali, Z.; Zahid, M. The Awareness and Impact of Carbon Capture and Storage (CCS) on Climate Change in Malaysia. *Int. J. Soc. Ecol. Sustain. Dev. (IJSESD)* **2018**, *9*, 13–27. [[CrossRef](#)]
95. Darman, N.; Harun, A.R. Technical challenges and solutions on natural gas development in Malaysia. In *The Petroleum Policy and Management (PPM) Project 4th Workshop of the China-Sichuan Basin Case Study*; Petroliaam Nasional Berhad (PETRONAS): Kuala Lumpur, Malaysia, 2006.
96. Bavoh, C.B.; Khan, M.S.; Ting, V.J.; Lal, B.; Ofei, T.N.; Ben-Awuah, J.; Ayoub, M.; Shariff, A.B.M. The Effect of Acidic Gases and Thermodynamic Inhibitors on the Hydrates Phase Boundary of Synthetic Malaysia Natural Gas. In *IOP Conference Series: Materials Science and Engineering*; IOP Publishing: Bristol, UK, 2018; Volume 458, p. 012016.
97. Isa, M.F.M.; Azhar, M.A. Meeting technical challenges in developing high CO<sub>2</sub> gas field offshore. *24th WGC Buenos Aires Argent.* **2009**, 5–9.

98. Wang, H.; Liu, Y.; Li, J. Designer Metal–Organic Frameworks for Size-Exclusion-Based Hydrocarbon Separations: Progress and Challenges. *Adv. Mater.* **2020**, 2002603. [[CrossRef](#)] [[PubMed](#)]
99. Xiang, Z.; Leng, S.; Cao, D. Functional group modification of metal–organic frameworks for CO<sub>2</sub> capture. *J. Phys. Chem. C* **2012**, *116*, 10573–10579. [[CrossRef](#)]
100. Trickett, C.A.; Helal, A.; Al-Maythaly, B.A.; Yamani, Z.H.; Cordova, K.E.; Yaghi, O.M. The chemistry of metal–organic frameworks for CO<sub>2</sub> capture, regeneration and conversion. *Nat. Rev. Mater.* **2017**, *2*, 1–16. [[CrossRef](#)]
101. Chen, T.; Wang, P.; Wang, N.; Sun, C.; Yang, X.; Li, H.; Zhou, G.; Li, Y. Separation of three polar compounds from *Rheum tanguticum* by high-speed countercurrent chromatography with an ethyl acetate/glacial acetic acid/water system. *J. Sep. Sci.* **2018**, *41*, 1775–1780. [[CrossRef](#)]
102. Razavi, S.A.A.; Morsali, A. Linker functionalized metal-organic frameworks. *Coord. Chem. Rev.* **2019**, *399*, 213023. [[CrossRef](#)]

**Publisher’s Note:** MDPI stays neutral with regard to jurisdictional claims in published maps and institutional affiliations.



© 2020 by the authors. Licensee MDPI, Basel, Switzerland. This article is an open access article distributed under the terms and conditions of the Creative Commons Attribution (CC BY) license (<http://creativecommons.org/licenses/by/4.0/>).